Gold Bulletin
Volume 43 No 2 2010

Selective Laser Melting (SLM) of pure gold

Mushtaq Khan* and Phill Dickens
www.goldbulletin.org

Abstract

This work presents an investigation into the Selective Laser Melting (SLM) of 24 carat gold (Au) powder with a mean particle size of 24µm. An SLM 100 system was used which is intended for production of highly detailed and intricate parts. Gold powder was tested for its properties such as tap density, Particle Size distribution (PSD) and reflectance etc. A suitable processing window was identified and gold cubes were produced using these parameters. Gold cubes were also checked for their internal porosity and mechanical properties.

Additive Manufacturing Research Group (AMRG), Wolfson School of Mechanical and Manufacturing Engineering, Loughborough University, LE11 3TU, Loughborough, Leicestershire, UK

* *Corresponding author: E-mail: mkhan_nust@yahoo.com, Tel: +44 (0) 1509 263171*

Introduction

Laser based Rapid Manufacturing (RM) processes such as selective laser sintering (SLS), Laser Engineered Net Shaping (LENS^{TM}), Direct Light Fabrication (DLF), Direct Metal Laser Sintering (DMLS) and Selective Laser Melting (SLM) have given greater flexibility in the manufacturing of complex 3D metallic parts. As compared to the sintering of powder in some other RM processes, the complete melting of powder in SLM could produce parts with much higher density and strength. SLM has already been successfully applied to process aluminium, copper, iron, stainless and tool steel, chromium, nickel alloys, titanium and composites of these materials [1-9]. Gold has been used for ornaments for centuries; however, very little work has been published [10] on the laser melting of precious metals like gold and its alloys.

This research work presents an initial investigation into the Selective Laser Melting 24 carat gold powder.

Material properties

A 24 carat gold powder (mean particle size of 24µm) manufactured using the gas atomization process for processing by an SLM 100 system. Gold powder was checked for its tap density according to ASTM B527 (1993) [11] and BS EN ISO 3953 (1995) [12] standards.

From its un-compacted state of 9.5g/cm^2, the gold powder compacted very quickly to 10.3g/cm^2. As the SLM process is a layer-by-layer process, the powder bed density or green density of the layers play an important role in the density of the final part. Zhu et al [13] proved that green density of the powder bed directly influences the final density of the sintered parts. Scanning Electron Microscope (SEM) images of the gold powder are presented in Fig 1. The gold particles were found to have a predominantly spherical shape but the smaller powder particles combined to form larger agglomerates. This agglomeration of gold powder reduced the powder flowability and hindered the powder deposition process. This problem was rectified by designing and developing a new powder deposition system and build platform which is discussed in detail in the next section.

Gold in the form of sheet and coatings is known to be very reflective in nature [14]. However powdered gold was observed to behave differently. The reflectance of these materials presented in this section was measured by the Diffuse Reflectance Infrared Fourier Transform Spectroscopy (DRIFTS) technique. This technique is especially designed for powered materials. The gold powder was found to be much more reflective (85%) in the infrared range (1060-1090nm) as compared to the other materials

Figure 1

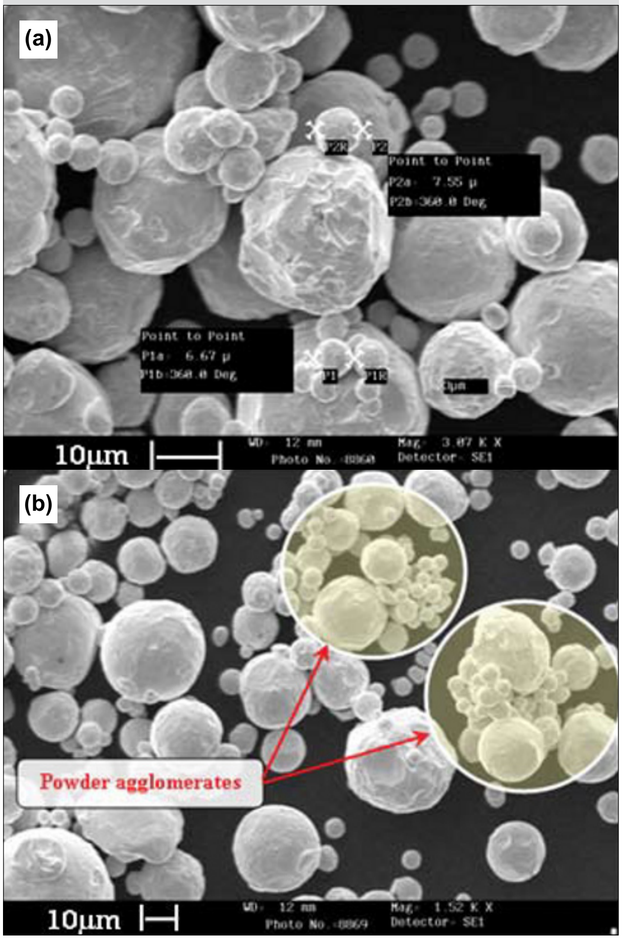

SEM images of un-sintered gold powder

such as copper (71%), H13 tool steel (39%), stainless steel (40) and Al12Si (35%).

When the radiation contacts a levelled powder surface, a portion strikes the particles lying directly on the top surface, while another portion penetrates between the pores to reach the interior of the powder (Fig 2). The radiation is repeatedly reflected between particles located at deeper levels in the powder bed which function as blackbodies i.e. these particles intensively absorb the radiation through multiple reflections [15]. The particles of several surface monolayers undergo heating by the incident laser radiation and the subsequent propagation of heat from the initially heated particles occurs via normal heat conduction methods. Fig 4 shows this phenomenon of radiation-material interaction where I_o is the incident radiation, Q_c is the heat transfer through conduction and I_r is the reflected radiation.

Selective Laser Melting (SLM) process and system

The MTT Technologies Group SLM 100 system uses a 50 watt continuous wave ytterbium doped infrared fibre laser in the Infrared range of 1070nm to 1090nm wavelength. The SLM 100's scanning system incorporates an f-theta lens and uses the same layered based techniques as the majority of other Solid Freeform Fabrication (SFF) processes. In the SLM 100, a wiper spreads a single layer of powder on the surface of a 125mm diameter steel substrate followed by the fiber laser scanning a single cross-sectional layer of the desired part.

Figure 2

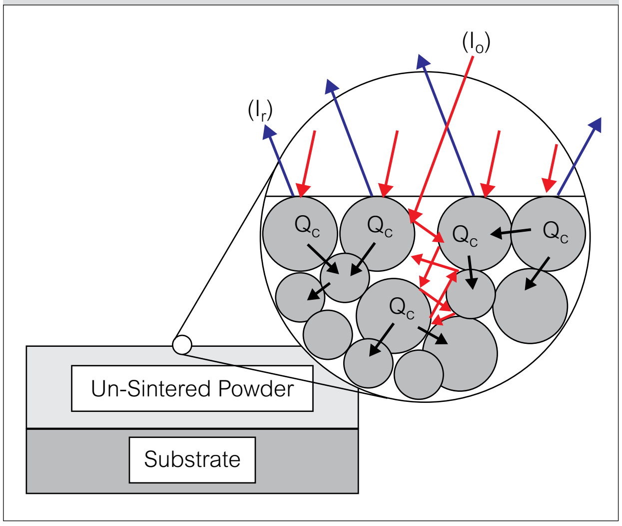

Radiation absorption and reflection from a powder bed

Figure 3

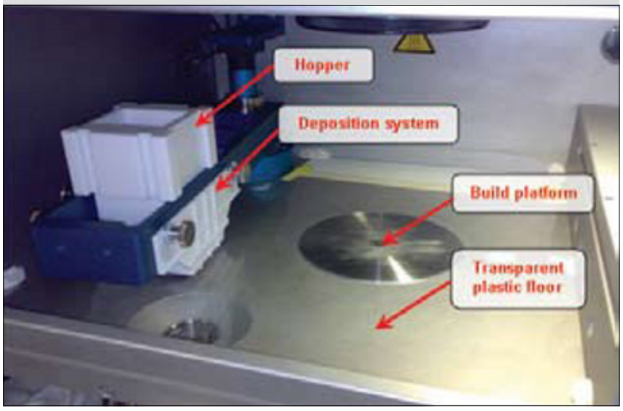

New deposition system and build platform installed inside the SLM 100 chamber

This process is repeated multiple times to create 3-dimensional metallic parts. A very small laser spot size and smaller build area makes the SLM 100 greatly suitable for highly detailed and customized small parts such as jewellery items etc from precious metal and alloys.

The SLM 100 system has a circular bed of 125mm in diameter and 80mm in z-direction. This build platform is very small compared to other commercial systems but due to the small quantity of gold powder available for this research a much smaller build platform was desirable. A new deposition system was developed in such a way that it was suitable for small quantities of gold powder, fitted well into the existing SLM 100 chamber and eliminated the deposition problems associated with poor flowability of gold powder. The new build platform was 15mm in diameter and 20mm in the z-direction. Fig 3 shows the new deposition system incorporated into the existing SLM 100 chamber replacing the large deposition system and build platform.

Selective Laser Melting (SLM) of gold (Au)

Before a material is qualified to be processed using SLM, the suitable processing parameters are identified. For this research, suitable processing parameters were selected and their ranges were identified. Thin layers of gold powder 100µm in thickness were deposited on the stainless steel substrate and single lines were scanned using different combinations of laser power and scan speed settings within their ranges. A powder bed temperature of 100ºC was maintained for all experiments.

Fig 4 shows the complete processing window for 24 carat gold powder. This processing window can be divided into five different zones/regions based on the quality of melt of the gold powder. These zones are: *Balling, Good Melting, Unstable Melt, Weak Sintering and Very Little Sintering*.

Balling is known to occur when the molten material forms small spherical balls instead of spreading evenly over the underlying surface to form beads (semicircular line of solidified molten material). If the length (L) to diameter (D) ratio of the melt pool is

Figure 4

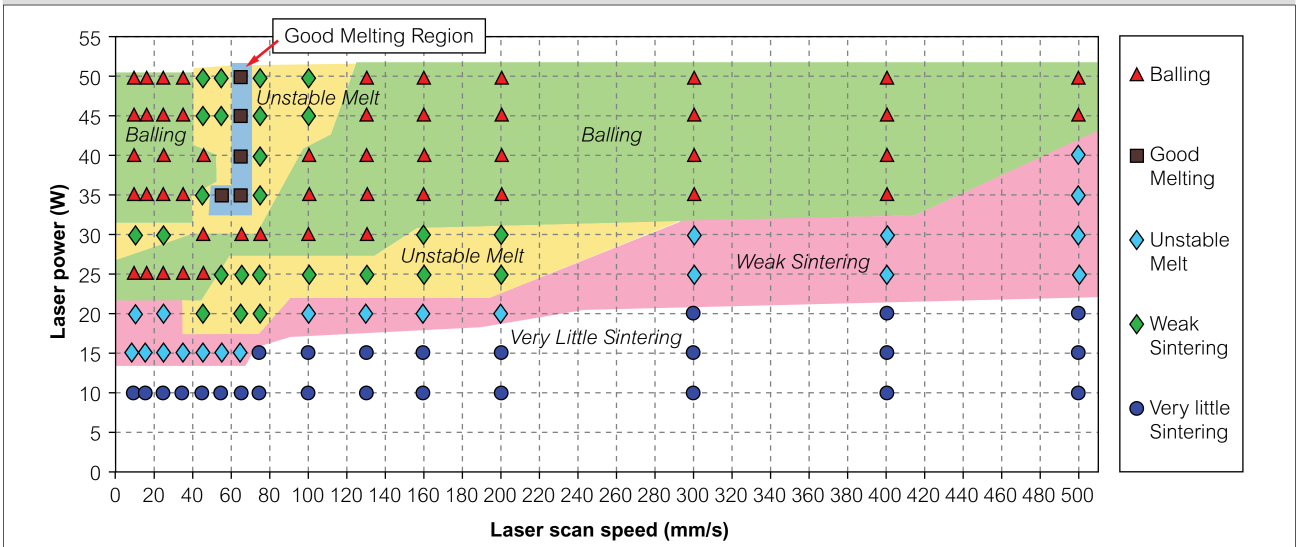

Processing window of gold powder

Figure 5

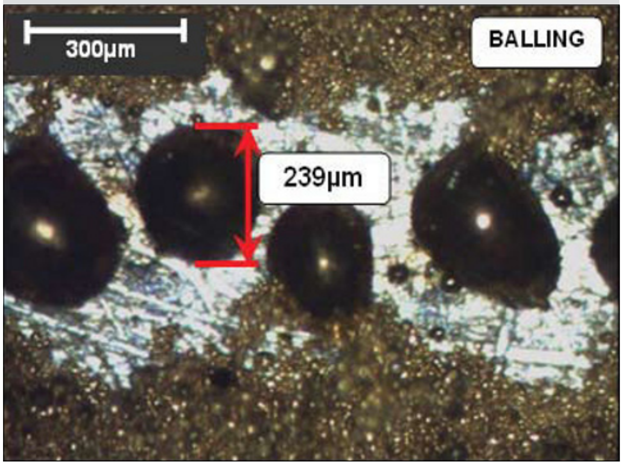

Balling occurred during SLM of gold at 50W laser power and 25mm/s scan speed

greater than 2.1 then the molten metal would break up into small droplets instead of a continuous line [4]. The balling observed at higher scan speeds could have been due to the increase in the length of the melt pool and a reduction in the melt pool width thus increasing the L/D ratio over 2.1 and destabilising the melt pool. At low scan speeds, the molten material has much greater time to be in the molten state compared to higher scan speeds. Therefore, balling at low scan speeds could be due to the high energy input and greater time available for the molten metal to split into smaller droplets (also called break-up time) before it could re-solidify. Fig 5 shows balling observed with laser melting of gold. The large droplet formation and large spacing in between these droplets (Fig 5) also suggests an increase in the break-up time of the molten metal [16].

Figure 6

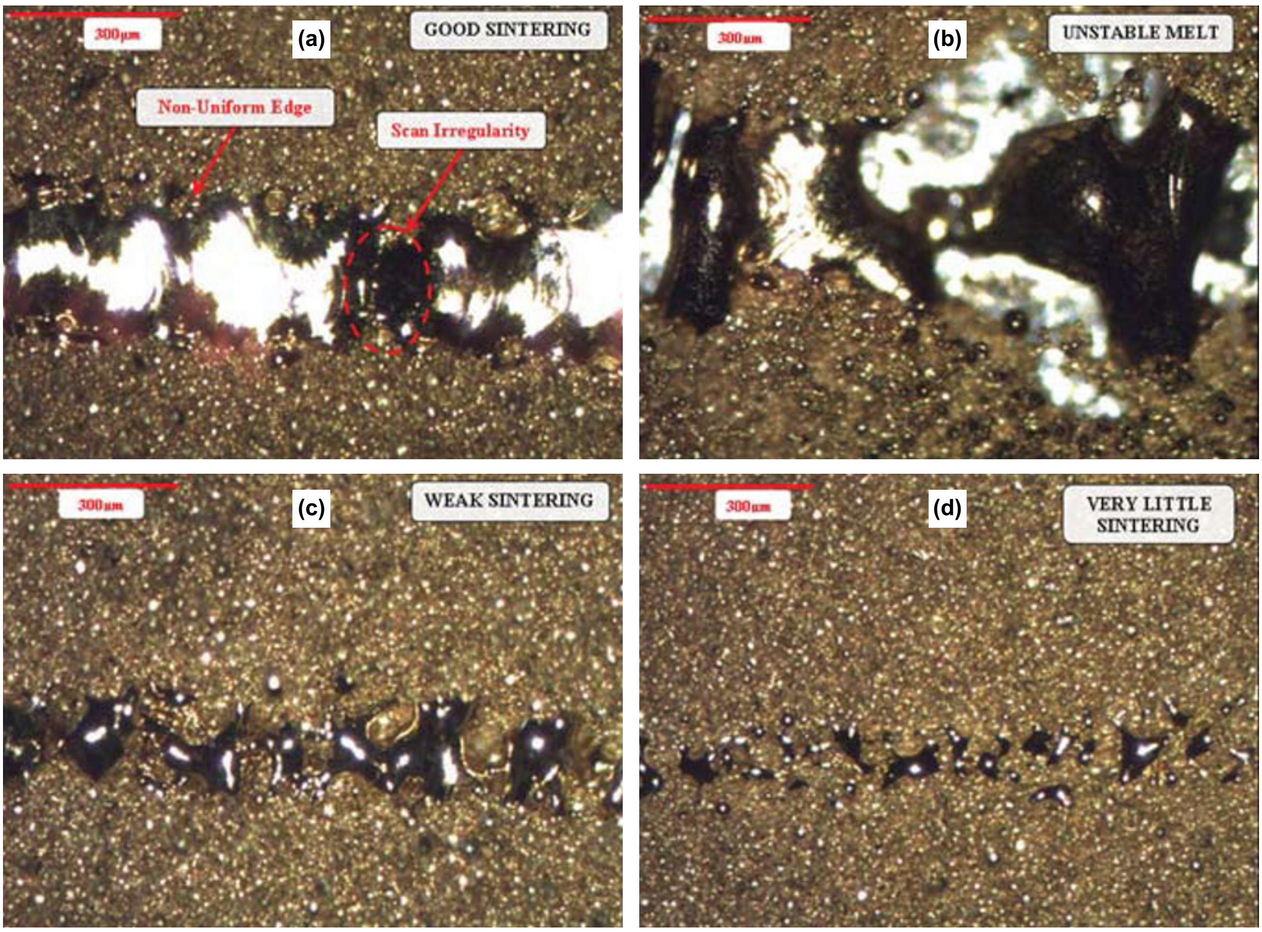

SLM of gold (a) good melting at 50W laser power and 65 mm/s scan speed (b) unstable melt at 50W laser power and 45 mm/s scan speed (c) weak sintering at 15W laser power and 25 mm/s scan speed and (d) very little sintering at 10W laser power and 10 mm/s scan speed

Fig 6a, b, c and d show example from the good melting, unstable melt, weak sintering and very little sintering scans from these regions. The gold powder completely melted in the good melting and unstable melt region but in the unstable melt region, the melt pool solidified into an irregular shape whereas good melting region showed good bead formation. The gold powder could not be completely melted in the weak sintering and very little sintering regions.

From the processing window of gold powder, a laser power of 50W and scan speed of 65mm/s was selected from the good sintering region as the optimum parameters. Gold cubes of 4x4x4 mm in size were produced with these optimum parameters using the new deposition system and build platform. An SEM image of a gold cube is shown in Fig 7.

Figure 7

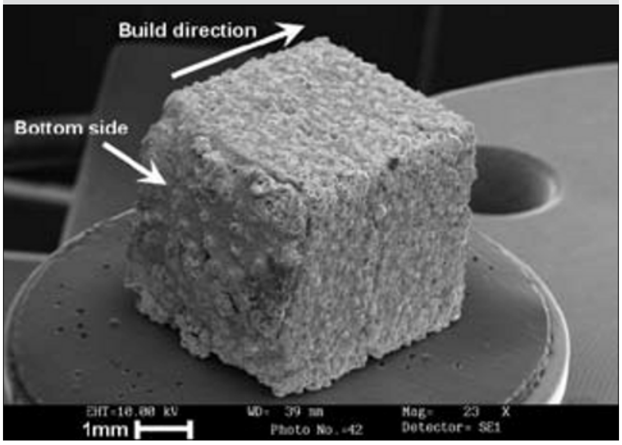

SEM image of gold cube

Analysis of gold cubes

Gold cubes were analysed for internal porosity and microhardness. The density of the gold cubes was analysed by an optical method. These gold cubes were mounted in epoxy resin and grounded using different grades of silicon carbide papers. Optical images were taken from the cross-section of each of these gold cubes and analysed to calculate the percentage of porosity in each cross-section. Table 1 shows the parameters used to study the effect on porosity with the results shown in Fig 8.

The internal porosity was at minimum (12.5%) for the optimum scan speed of 65mm/s. Fig 9a, b and c shows the original, grey scale and processed image of the cross section of the gold cube manufactured at 50W laser power and 65mm/s scan speed.

It was also observed that most of the porosity was the inter-layer. The high porosity between the layers suggests less heat was transferred to the underneath layers, thus resulting in weak bonding between consecutive layers. The high reflectivity of gold powder (approximately 85%) could be the

Figure 8

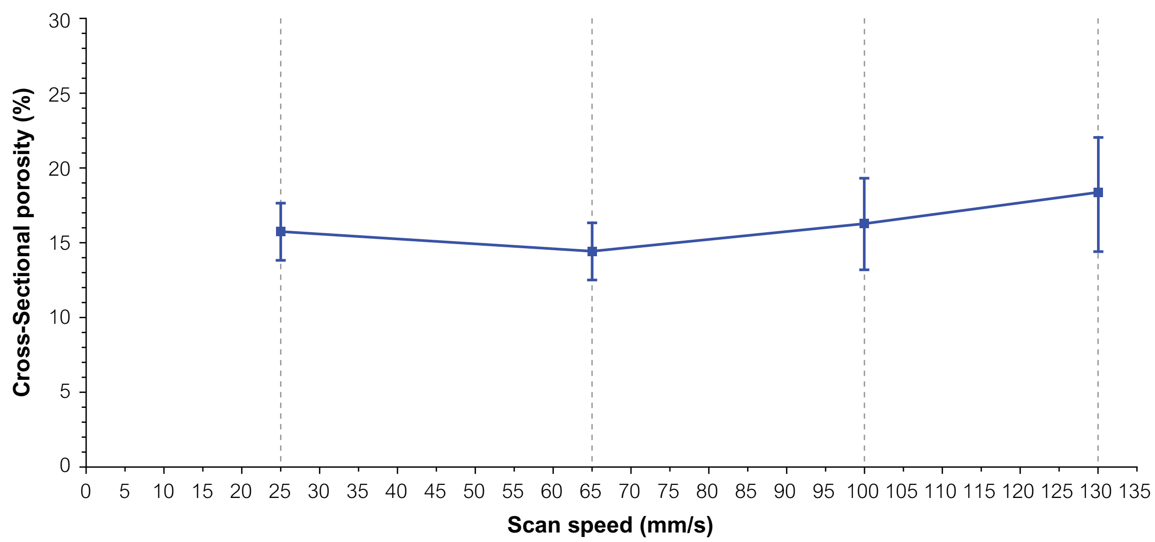

Internal porosity for gold cubes for different scan speeds

Table 1: Parameters settings for manufacturing gold cubes

Sample #	Laser power (W)	Scan speed (mm/sec)	Hatch distance (µm)	Layer thickness (µm)	Hardness (HV)
1	50	25	80	100	24.6
2	50	65	80	100	29
3	50	100	80	100	21.5
4	50	130	80	100	22.3

Figure 9

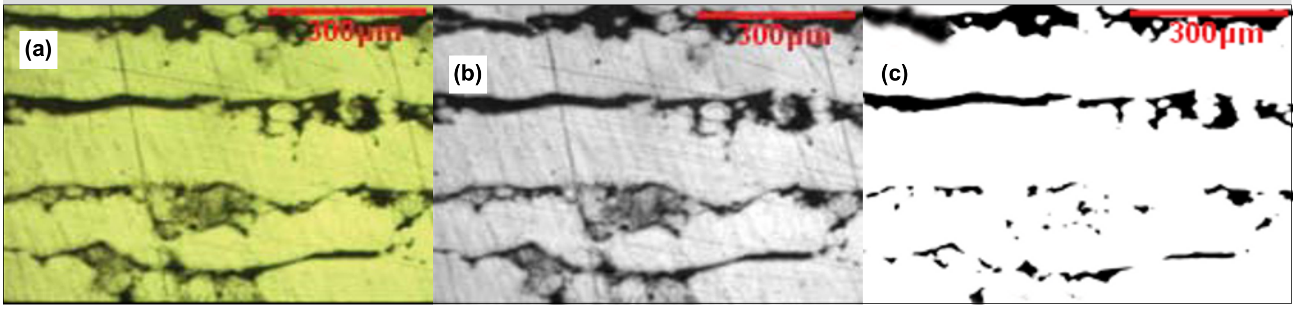

Gold cubes cross section images (a) original image (b) grey scale image (c) processed image (12.5% porosity)

possible reason for the low energy transferred to the underlying layers. This reflectivity also increases as the gold powder melts and forms a solid layer during the laser processing, thus further reducing the amount of energy absorbed. Due to this reason there was very little melting and most of the porosity was observed in the region between the layers. The Inter-layer porosity reduced the bonding between the layers and created layer delamination in the final part.

As the laser power and scan speed was fixed at 50W and 65mm/s respectively from the good melting region, the layer thickness and hatch distance were further reduced to increase the amount of energy input.

Fig 10 shows the effect of layer thickness on the internal porosity of gold cubes. It was observed that there was no difference in porosity when the layer thickness was reduced from 100µm to 75µm; however, the porosity was reduced from 14.4% to 10.4% when the layer thickness was reduced from 75µm to 50µm. Due to the cohesive nature of gold powder, a layer thickness below 50µm could not be deposited with the new deposition system.

Figure 10

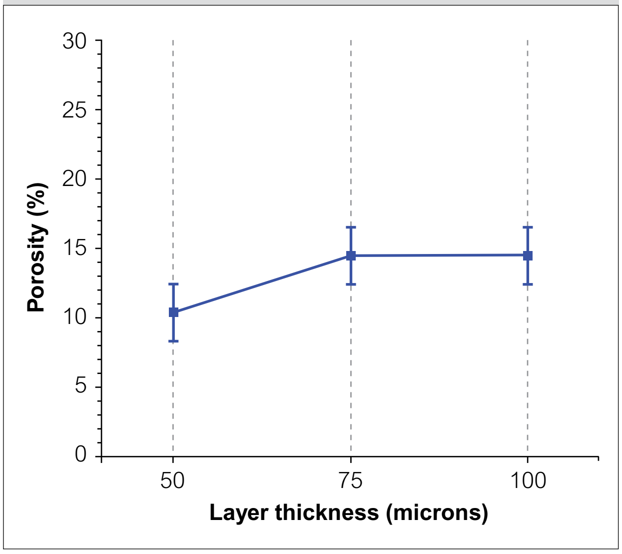

Porosity vs Layer thickness

The hatch distance was varied from 80 to 60 and 40µm thus increasing the laser overlap. Fig 11 shows that hatch distance had almost a negligible effect on the internal porosity of gold cubes. Although the reduction in hatch distance increased the energy density, it was still not enough to have a significant influence on the depth to which the heat energy

Figure 11

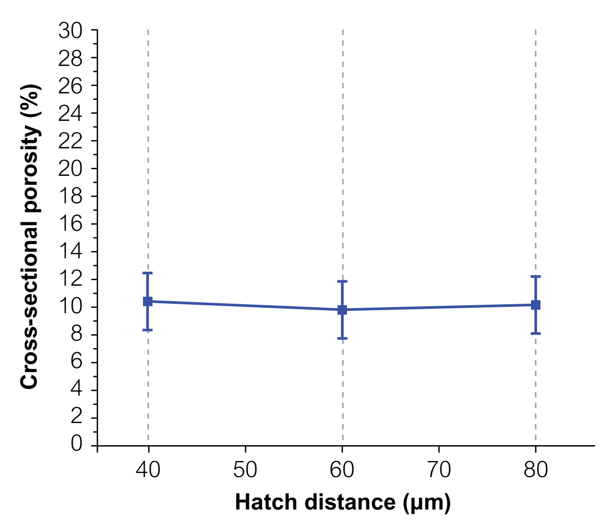

Porosity vs hatch distance

Figure 12

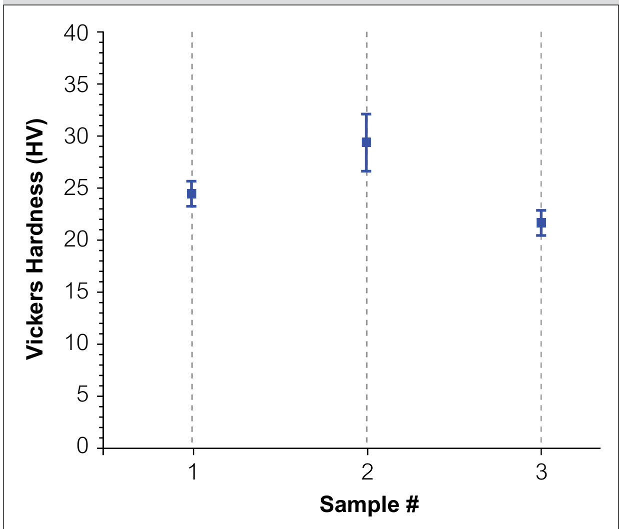

Microhardness of gold cubes

was transferred. This left the area between the two layers un-melted; hence the porosity remained almost the same.

Three gold cubes produced at different scan speeds were also checked for their hardness. Microhardness testing was performed using a Mitutoyo HM200 machine. The microhardness of the gold cubes manufactured at 25, 65 and 100mm/s (Fig 12) was found to be consistent with the hardness values of 24 carat gold (25HV).

Conclusions

Gold powder was found to be cohesive in nature due to the agglomerates in the powder and highly reflective in the infrared range as compared to other materials processed using SLM. The processing window of gold powder showed five different regions of degree of melting of gold. The good melting region was found to have completely melted gold powder with good bead formation.

Gold cubes were manufactured using the optimum parameters (50W laser power and 65mm/s scan speed). The porosity in gold cubes was observed to be predominantly inter-layer porosity. This inter-layer porosity was possibly associated with the lower amount of energy absorbed by the gold powder thus not completely fusing powder to the previous layer. Layer thickness was reduced from 100µm to 50µm but this had little effect on the density of the gold cubes. Hatch distance was observed to have almost negligible effect.

About the authors

Mushtaq Khan is a PhD researcher in the Additive Manufacturing Research Group (AMRG) at Loughborough University UK. His research focuses on the Selective Laser Melting (SLM) of Gold (Au).

Phill Dickens (Professor of Manufacturing Technology)
Phill Dickens is the Pro-Vice-Chancellor (Enterprise) and leads the University's core strategies of building on its knowledge transfer achievements and exploiting further its intellectual assets. As Pro-Vice-Chancellor (Enterprise), Phill directs all activities within the Enterprise Office and is also responsible for maximising the scope for innovation and creativity in the expansion of this area. Phill started working on Rapid Prototyping in 1991 at the University of Nottingham and developed the concept into Rapid Manufacturing. His broad interests and expertise are in the field of Rapid Manufacturing Processes.

References

1 F. Abe, K. Osakada, M. Shiomi, K. Uematsu, M. Matsumoto, *J. of Materials Processing Technology*, 2001, **111**, 210

2 W.N. Su, P. Erasenthiran, P.M. Dickens, *J. of Mechanical Engineering Science*, 2003, **217**, 127

3 F. Abe, E.C. Santos, Y. Kitamura, K. Osakada, M. Shiomi, *J. of Mechanical Engineering Science*, 2003, **217**, 119

4 J.P. Kruth, L. Froyen, J. Van Vaerenbergh, P. Mercelis, M. Rombouts, B. Lauwers, *J. of Materials Processing Technology*, 2004, **149**, 616

5 S. Pogson, P. Fox, W. O'Neill, C.J. Sutcliffe, *Materials Science and Engineering A*, 2004, **386**, 453

6 E.C. Santos, K. Osakada, M. Shiomi, Y. Kitamura, F. Abe, *J. of Mechanical Engineering Science*, 2004, **218**, 711

7 T.H.C. Childs, *Proc. IMechE*, 2005, **219**, 379

8 K. Mumtaz, N. Hopkinson, P. Erasenthiran, *Solid Freeform Fabrication Symposium*, 2006, 220, Austin, Texas, USA

9 I. Yadroitsev, L. Thivillon, P. Bertrand, I. Smurov, *App. Surface Science*, 2007, **254**, 980

10 L. Thorsson, *Proceeding of 1st International Conference on Rapid Manufacturing*, 2006, 5-6 July, Loughborough, UK

11 American Society for Testing Materials, *Standard Test Method for Determination of Tap Density of Metallic Powders and Compounds*, 2006, ASTM B527

12 British Standard, *Metallic Powders – Determination of Tap Density*, 1995, BS EN ISO 3953

13 H.H. Zhu, J.Y.H. Fuh, L. Lu, *International Journal of Machine Tools and Manufacture*, 2007, **47**, 294

14 J. Mohelnikova, *Construction and Building Materials*, 2009, **23**, 1993

15 N.K. Tolochko, Y.V. Khlopkov, S.E. Mozzharov, N.V. Sobolenko, I.A. Yadroitsev, *Powder Metallurgy and Metal Ceramics*, 1997, **36**, 433

16 M. Rombouts, J.P. Kruth, L. Froyen, P. Mercelis, (2006), CIRP *Annals - Manufacturing Technology*, **55**, 187